EASI SMR

D7.4 Analysis of the code benchmarking for the LDR-50-lite core at BOC conditions

Riku Tuominen (VTT), Yuri Bilodid (HZDR), Jeremy Bousquet (GRS)

1. Document information

Grant Agreement Number	n°101164810
Project Title	Ensuring Assessment of Safety Innovations for SMR
Project Acronym	EASI-SMR
Project Coordinator	Nicolas Sobecki, EDF
Project Duration	1 September 2024 – 31 August 2028 (48 months)
Related Work Package	WP7 Advanced Core Physics Studies of Boron-Free SMR-cores
Lead Organisation	VTT
Contributing Partner(s)	HZDR, GRS
Submission Date	24.04.2026
Dissemination Level	Public

2. History

Date	Submitted by	Reviewed by	Version (Notes)
24.03.2026	R. Tuominen		Initial release
30.03.2026		V. Sanchez-Espinoza	
03.04.2026		N. Sobecki	
14.04.2026	R. Tuominen	N. Sobecki (EDF)	Revision
24.04.2026	N. Sobecki (EDF)	O. Fauchet, A. Paul	Final

Co-funded by the European Union
UK Research and Innovation
The Research Council of Norway
Project funded by

Table of Contents

List of Figures

List of Tables

Co-funded by the European Union
UK Research and Innovation
The Research Council of Norway
Project funded by

3. Summary

This deliverable describes the modelling of the initial core of LDR lite at beginning of cycle conditions. The calculations models were built based on the specifications reported in deliverable D7.2. The modelling of the fresh core serves as an important verification step for the models before moving on to depletion calculations in Task 7.5 and to transient calculations in Task 7.6.

Two neutronics only states, namely all-rods-out state and a critical state with predefined control rod insertions, were modelled along with a hot full power state with neutronics-thermal hydraulics coupling. Diffusion based results were calculated by VTT with the nodal diffusion code Ants and Ants coupled to subchannel code SUBCHANFLOW, by HZDR with the reactor simulator DYN3D and by GRS with the finite element neutronics code FENNECS and FENNECS coupled to systems code ATHLET. These results were compared against reference results calculated by VTT with the Monte Carlo transport code Serpent and a coupling between Serpent and subchannel code SUBCHANFLOW. The effect of the number of energy groups used in the nodal diffusion solution was studied by repeating the Ants and DYN3D simulations with 2, 4 and 8 energy groups.

The best overall agreement with the reference results were obtained using Ants and DYN3D with 2 energy groups. Increasing the number of energy groups showed no notable improvements and, in some cases, increased the differences compared to the reference. With 2 energy groups the differences were limited to 200 pcm in core reactivity, 2 % in assembly powers and 7 % in pin powers.

Larger differences were observed for FENNECS compared to Ants and DYN3D. FENNECS underestimated the core reactivity by approximately 800-900 pcm in the three modelled states. Maximum differences in the assembly powers were 3.9 %, 5.9 % and 4.4 % for the all-rods-out, critical and hot full power states, respectively. FENNECS does not currently support pin power reconstruction and therefore pin powers were not evaluated with FENNECS. A possible explanation for the larger discrepancies in FENNECS results is the inaccurate modelling of the radial reflector which requires improvements.

4. Keywords

LDR lite, BOC, HFP, Ants, DYN3D, FENNECS, Serpent

Co-funded by the European Union
UK Research and Innovation
The Research Council of Norway
Project funded by

5. Abbreviations and acronyms

Acronym	Description
ARO	All Rods Out
BOC	Beginning Of Cycle
HFP	Hot Full Power
RMS	Root Mean Square
SCF	SUBCHANFLOW
TH	Thermal Hydraulics
WP	Work Package

Co-funded by the European Union
UK Research and Innovation
The Research Council of Norway
Project funded by

6. Introduction

In WP7 of the EASI-SMR project, two light water boron free SMR cores, PRATIC and LDR lite, are modelled. LDR lite is a public representation of the LDR-50 reactor concept. The work with LDR lite started in Subtask 7.1.2 with the definition of the beginning of the initial cycle core specifications reported in deliverable D7.2 (Valtavirta & Tuominen, 2025). In this deliverable, the beginning of cycle (BOC) core is modelled based on these specifications. This is an important verification step for the calculation models before moving on to depletion calculations in Task 7.5 and to transient calculations in Task 7.3.

Two neutronics only states and a HFP state with neutronics-thermal hydraulics (TH) coupling are analyzed at BOC. Diffusion based solutions are provided by VTT with the nodal diffusion code Ants and Ants coupled to subchannel code SUBCHANFLOW (SCF), by HZDR with the reactor simulator DYN3D and by GRS with the finite element neutronics code FENNECS and FENNECS coupled to systems code ATHLET. The results obtained with these codes are compared against reference results calculated by VTT using the Monte Carlo transport code Serpent for the neutronics only states and with Serpent/SCF coupled code system for the HFP state. The effect of the number of energy groups on the results is studied using Ants and DYN3D by repeating the simulations with 2, 4 and 8 energy groups. The Ants and DYN3D results for the BOC state are also presented in a conference paper (Tuominen & Bilodid, 2026).

7. LDR lite core

The LDR lite is a public representation of the LDR-50 small modular reactor initially developed at VTT Technical Research Centre of Finland Ltd and now being commercialized by Steady Energy Oy. This low temperature and low pressure 50 MWth light water reactor has been designed for low temperature heat production applications. The design features natural circulation-driven primary circuit, in-vessel control rod drives, and self-pressurization. Passive decay heat removal is achieved through a dual vessel design. Since the coolant in the core is without soluble boron, long term reactivity control is achieved by using burnable absorbers and grey control rods. The active height of the core is 100 cm, and it contains 37square fuel assemblies of type 17x17.

The core loading pattern of the initial core of LDR lite is presented in Figure 1. There are six different fuel assembly types, four of which contain gadolinium. The fuel assemblies are surrounded radially by a stainless-steel reflector. Control rods are present in each assembly, and they have been divided into eight groups with four regulating and four safety groups. Control rod group locations are illustrated in Figure 2. More detailed description of the core is available in D7.2 (Valtavirta & Tuominen, 2025).

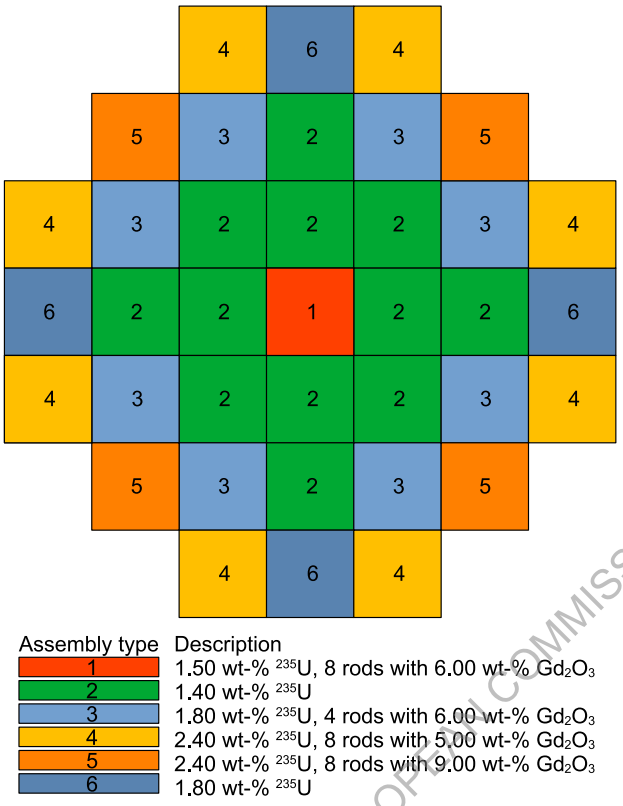

Figure 1. Core loading pattern of the initial core. Source: (Valtavirta & Tuominen, 2025)

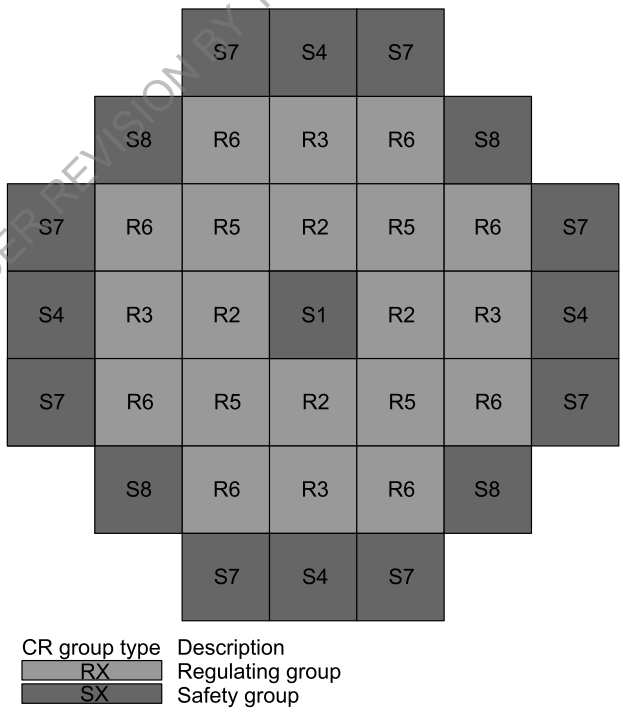

Figure 2. Control rod group locations. Source: (Valtavirta & Tuominen, 2025)

8. Description of the analyses at BOC

The analysis of the initial core of LDR lite at BOC (Valtavirta & Tuominen, 2025) consisted of the modelling of two neutronics only states with fixed TH conditions and HFP state with neutronics-TH coupling. The neutronics only states were the all-rods-out (ARO) state and a critical state with predefined control rod group insertions. These insertions were obtained by running a simple algorithm aiming to minimize the radial peaking of the power distribution. The insertions are presented in Table 1. The fixed TH conditions are given in Table 2 and they represent the core average values at nominal power. The neutronics only states were modelled without xenon.

Table 1. Insertions of the control rod groups for the critical state.

Group	Insertion (%)
S1	0
R2	76
R3	86
S4	0
R5	75
R6	72
S7	0
S8	0

Table 2. Fixed TH conditions for the ARO and critical states.

Property	Value	Unit
Fuel temperature	525	K
Coolant temperature	410	K
Coolant density	0.92915	g/cm^3

Control rod group positions used in the HFP state are given in Table 3. They were iterated in a similar manner as in the critical state. TH boundary conditions for the HFP state are specified in Table 4. In the modelling of the fuel behavior, the fixed thermophysical properties presented in Table 5 were utilized. Equilibrium xenon was used.

Table 3. Insertions of the control rod groups for the HFP state.

Group	Insertion (%)
S1	0
R2	67
R3	64
S4	0
R5	66
R6	56
S7	0
S8	0

Table 4. TH boundary conditions for the HFP state.

Parameter	Value	Unit	Note
Power	50	MW	
Core inlet mass flow rate	237.12	kg/s	Uniformly distributed to all fuel assemblies
Core inlet temperature	379	K	
Core outlet temperature	0.755	MPa	

Table 5. Fixed thermophysical properties for the fuel and the cladding.

Parameter	Value	Unit
Fuel density	10.295	g/cm^3
Fuel thermal conductivity	5.2	W/(m·K)
Fuel specific heat capacity	290	J/(kg·K)
Cladding density	6.55	g/cm^3
Cladding thermal conductivity	14.7	W/(m·K)
Cladding specific heat capacity	310	J/(kg·K)
Gap conductance	5000	W/(m^2·K)

In both the ARO and critical states effective multiplication factors along with axial, assembly and pin power distributions calculated with the reduced order codes were compared against Serpent reference results. In addition, fuel/coolant temperature reactivity coefficients in the critical state and control rod group worths were compared. The reactivity coefficients were calculated based on the variations given in Table 6 using the following procedure:

1. Apply variation to fuel temperature or coolant temperature and density.
2. Calculate new effective multiplication factor.
3. Evaluate reactivity coefficient in pcm/K as:

$$\frac{\left(\left(1-\frac{1}{k_{eff,var}}\right)-\left(1-\frac{1}{k_{eff,nom}}\right)\right)}{\Delta T} \times 10^5,$$

where ΔT is the change in fuel or coolant temperature in K, and $k_{eff,nom}$ is the effective multiplication factor for the nominal critical state and $k_{eff,var}$ is the effective multiplication factor after the variation was applied.

Table 6. TH variations for the evaluation of reactivity coefficients in the critical state.

Reactivity coefficient	Fuel temperature (K)	Coolant temperature (K)	Coolant density (g/cm^3)
Fuel temperature	575	410	0.92915
Coolant temperature	525	430	0.91062

In the HFP state, effective multiplication factors along with axial, assembly and pin power distributions estimated with the reduced order codes were compared against Serpent reference results.

9. Calculation methods

9.1. Reference Monte Carlo solution with Serpent(-SCF)

Serpent (Leppänen;Valtavirta;Rintala;& Tuominen, 2025) is a Monte Carlo transport code developed at VTT. The code can be used for various applications such as group constant generation, photon transport, and multi-physics calculations. A key functionality for the multi-physics calculations has been the multi-physics interface which allows for bringing in temperature and density distributions to Serpent in a straightforward manner.

SUBCHANFLOW (Imke & Sanchez, 2012) is a subchannel thermal hydraulics solver developed at KIT. The code solves liquid-vapor mixture equations for the conservation of mass, momentum, and energy. In addition, SCF relies on the use of empirical correlations for evaluating pressure drop, heat transfer, void generation, etc. The fuel rods can be modelled with a simplified fuel behavior model.

The Serpent full core model was constructed according to the specifications presented in D7.2. The model used ENDF/B-VII.1 based cross section library. The model is illustrated in Figure 3 and in Figure 4.

In the estimation of effective multiplication factors and power distributions for the ARO and critical states 50 billion active neutron histories were simulated. Control rod group worths were evaluated with 5 billion active neutron histories. The standard deviation of the effective multiplication factor was less than approximately 1 pcm in all transport calculations. The assembly and pin power distributions were tallied over the entire core and averaged over the 45 degree symmetry sectors in post processing. In this averaging process the information about the statistical uncertainties of these distributions was lost. However, before the averaging the maximum relative statistical errors for the assembly and pin power distributions were approximately 0.01 % and 0.1 %, respectively. The maximum relative statistical errors for the axial power distributions were approximately 0.01 %.

Co-funded by the European Union
UK Research and Innovation
The Research Council of Norway
Project funded by

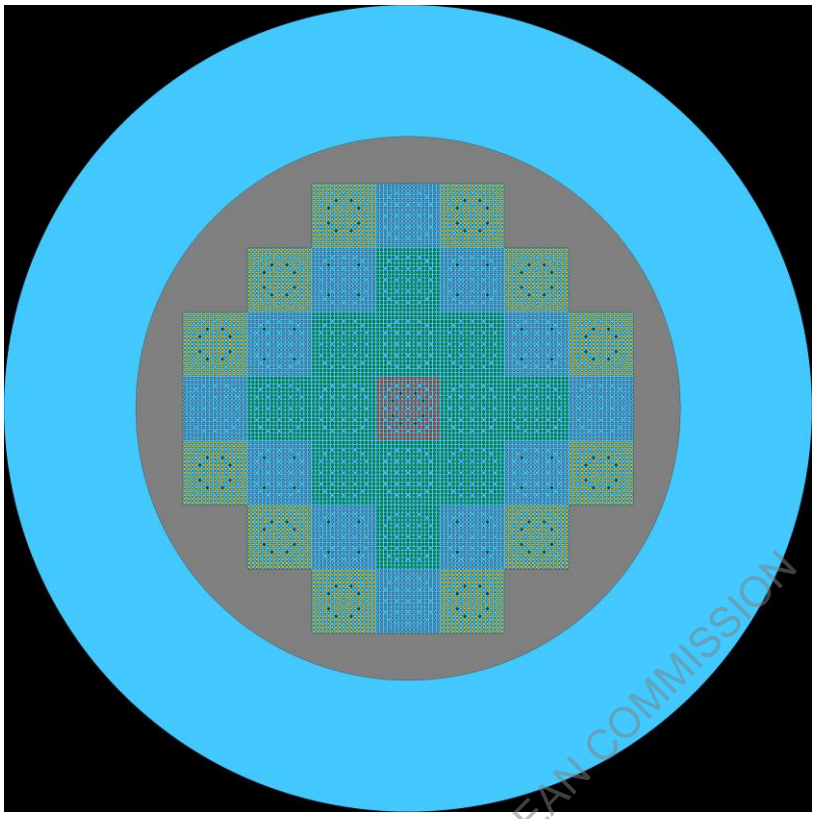

Figure 3. Radial geometry of the Serpent full core model.

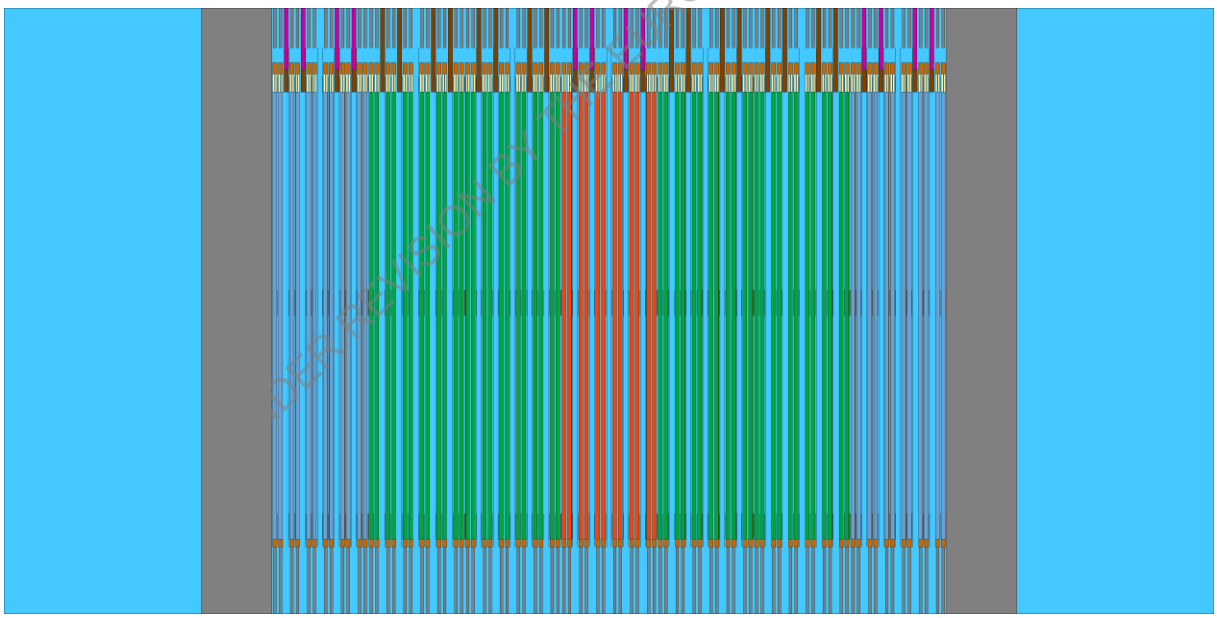

Figure 4. Axial geometry of the Serpent full core model.

The reference solution for the HFP state was calculated with the coupled Serpent-SCF code system. The codes were coupled within VTT's Kraken framework using the Cerberus multi-physics driver. The coupled calculation was run for 5 coupled iterations. On the last iteration the maximum absolute differences in the local fuel and coolant temperatures compared to previous iteration were approximately 0.2 K and 0.02 K, respectively. In order to have a rough estimate of the statistical uncertainty of the coupled solution, the coupled calculation was run two times, and the results were

Co-funded by the European Union
UK Research and Innovation
The Research Council of Norway
Project funded by

compared against each other. The difference between the two calculations in the effective multiplication factor was approximately 1 pcm. Maximum relative differences in the assembly, pin and axial power distributions were approximately 0.04 %, 0.3 % and 0.06 %, respectively.

In SCF the coolant flow was modelled on subchannel level and the fuel behaviour on pin-by-pin level. The fixed thermophysical properties for the fuel and the cladding presented in Table 5 were used. The inlet flow distribution in SCF was specified by setting the total inlet mass flow rate and using the set_flow_split_first_axial = on option, which divides the channel flow rates at the inlet to obtain an equal pressure drop across the first axial node for all channels. Therefore, the inlet flow rate distribution is slightly non-uniform. It should be noted that severe converge issues were encountered with the default upwards flow only (UPWA) solver and therefore, the SOLA solver was used. In the SCF manual this solver is described to be more robust for cases with small axial flow rates (Imke, 2019).

9.2. Group constant generation with Serpent for Ants and DYN3D

Group constants for both Ants and DYN3D were generated with Serpent using an ENDF/B-VII.1 based cross section library. Fuel assemblies were homogenized as 2D infinite lattice quarter assembly models with fundamental mode leakage correction. Fuel assembly discontinuity factors calculated directly by Serpent were used in both Ants and DYN3D. The axial reflector was homogenized using a single assembly 3D model and one assembly width of radial reflector was homogenized from a 2D full core model into quarter assembly sized regions. Diffusion coefficients for the fuel assemblies were generated with the Cumulative Migration Method (CMM) (Liu;Smith;& Forget, 2018) and in the reflector regions the diffusion coefficients were based on the out-scatter approximation with transport correction applied to ^{1}H in water. The energy groups structures used with DYN3D, and Ants are presented in Table 7.

The group constants were generated separately for the neutronics only states and for the HFP state. For the neutronics only states, they were generated directly for the state point specified in Table 2. For the HFP state the variation in the fuel assembly group constants due to variations in the thermal hydraulics conditions was taken into account with 9 branch calculations resulting from combining 3 fuel temperatures (low, nominal, high) with 3 moderator temperatures/densities (low, nominal, high). For the reflectors, the same 3 moderator branches were run.

In Ants, the dependency of the group constants on the thermal hydraulic conditions was represented by polynomials. In case of fuel assemblies, first and second order terms were used for the square root of the fuel temperature and the moderator density. In addition, a first order cross term was included. The reflector group constants were fitted with first and second order terms for the moderator density.

For Ants the discontinuity factors for the radial reflector nodes were evaluated based on heterogeneous surface fluxes tallied in the Serpent 2D full core calculation and

Co-funded by the European Union
UK Research and Innovation
The Research Council of Norway
Project funded by

homogeneous surface fluxes which were obtained from single node Ants calculations utilizing group constants and boundary conditions from the Serpent 2D full core calculation. As an additional step, for each node the reflector side discontinuity factor was corrected by the ratio of the fuel side infinite lattice assembly discontinuity factor and the fuel side full core evaluated discontinuity factor as suggested in (Smith, 2017).

In DYN3D, the dependency of the group constants on the thermal hydraulic conditions was represented by multi-dimensional tables. Local values of the group constants are estimated using local temperatures by linear interpolation between closest branch points.

For the first row of radial reflector, which directly interfaces with fuel, the discontinuity factors for DYN3D library are calculated as ratio of heterogeneous to homogeneous surface fluxes. Heterogeneous fluxes are obtained from Serpent 2D full core calculation, while homogeneous surface fluxes are obtained in post-processing by a separate diffusion solver, which applies the same nodal expansion as DYN3D, using Serpent full core surface currents of each reflector region as boundary conditions. For the second row of reflector nodes, discontinuity factors for neighboring first-row reflector regions are applied.

Table 7. Group boundaries for the energy group structures used with Ants and DYN3D.

2 groups	4 groups	8 groups
1e37 MeV	1e37 MeV	1e37 MeV
	821 keV	821 keV
	5.53 keV	5.53 keV
		4 eV
0.625 eV	0.625 eV	0.625 eV
		0.28 eV
		0.14 eV
		58 meV
0 eV	0 eV	0 eV

9.3. Ants(-SCF) nodal diffusion solution

Ants (Sahlberg & Rintala, 2018) is a multi-group nodal neutronics program capable of solving eigenvalue or fixed-source steady-state, depletion and time-dependent problems. The nodal diffusion solution methodology is based on a combination of the flux expansion nodal method (FENM) and the analytic function expansion nodal method (AFEN).

In the Ants model the active region was divided axially into 18 nodes. In addition, there was one node in both bottom and top reflectors. Radially the model consisted of the active core and one assembly-wide of radial reflector. 2x2 sub-nodalization was used in each assembly.

In order to simulate the HFP state a coupled calculation between Ants and SCF was run. The codes were coupled within VTT's Kraken framework using the Cerberus multi-physics driver. SCF solved the coolant flow and fuel behaviour on quarter assembly level i.e. with one channel/representative fuel rod for each quarter assembly. UPWA

algorithm was used in SCF since no convergence issues were encountered with the quarter assembly level solution.

9.4. DYN3D nodal diffusion solution

DYN3D is a 3D nuclear reactor core transient simulator developed at HZDR (Rohde, 2016). The code comprises neutron kinetics, thermal-hydraulics, and fuel rod solvers. The 3D multi-group neutron kinetics model is based on nodal expansion methods for the neutron flux calculation for various core geometries (cartesian, hexagonal, or on a trigonal grid). In DYN3D, thermal hydraulics are solved using a four-equation two-phase flow model for 1D parallel channels without crossflow between them, a boron transport model, and a fuel rod model. The fuel rod model comprises the solution of the 1D heat conduction equation and the thermal-mechanical modelling of the gas gap between the fuel and cladding.

The DYN3D model applied the same spatial discretization as the Ants model: 20 axial nodes and 2x2 sub-nodalization for each fuel assembly and assembly-size radial reflector region. The model utilized DYN3D's internal TH solver, representing the core as a set of 1D parallel two-phase flow channels, with a channel assigned to each quarter-assembly. Pin powers are obtained after the nodal solution has converged, using nodal surface fluxes as boundary conditions and pin power factors calculated in Serpent single assembly model.

9.5. Group constant generation with SCALE for FENNECS

Group constants required by the diffusion code FENNECS (Seubert, lo Muzio, Elts, & Bousquet, 2026) were generated with the module NEWT from SCALE (Wieselquist & Lefebvre, 2024) code package.

The SCALE Code System, developed at Oak Ridge National Laboratory (ORNL), provides tools for criticality safety, reactor and lattice physics, radiation shielding, spent fuel and radioactive source term characterization, and sensitivity and uncertainty analysis. NEWT (New ESC-based Weighting Transport code) is part of this package. It is a multigroup discrete-ordinates radiation transport computer code for 2D neutron transport calculations.

Inputs required for NEWT are generated by the core simulator KMACS (Kernsimulator, a Modular Adatable Core Simulation) (Zilly & Périn, 2018) developed at GRS. KMACS combines lattice codes, nodal diffusion codes with explicit thermal-hydraulics feedback and inventory codes into a nodal core simulator. The individual codes are steered and executed via Python modules. The results are stored in a central database which also serves data exchange and analysis.

All assembly types are modelled as full assemblies in SCALE-NEWT using the v7.1-56 library (ENDF/B-VII.1 library collapsed into 56 energy groups) twice: a model without spacer grid and another one where the spacer grid is homogeneously smeared into the

Co-funded by the European Union
UK Research and Innovation
The Research Council of Norway
Project funded by

moderator between the fuel pins and guide tubes as well as the inter-assembly gap, but not within the guide tube. The group constants were collapsed into a 2-energy-group structure (cut at 0.625 eV) like the 2-energy-structure used for DYN3D and Ants.

FENNECS was initially developed for analysis of innovative concepts with complex or non-regular geometries including Micro Modular Reactors (MMRs) (Bousquet, Seubert, & Henry, 2020) and Generation IV designs. FENNECS is still under development, especially for light water reactor analysis. To obtain better results in PWR analysis, FENNECS requires the application of Assembly Discontinuity Factors (ADF) (Henry, Bousquet, & Seubert, 2024) which are applied to all fuel assemblies as well as to all radial reflector types. These ADF are directly calculated by NEWT.

For bottom and top reflectors, the 2D system consists of a full horizontal assembly model next to a homogeneous mixture of all compositions of the entire reflector part.

The radial reflector model is a linear array of fuel assembly, stainless steel reflector and moderator with reflective boundary conditions at the north, west, and south boundary but vacuum boundary conditions in the east. Since the distance between fuel assembly, stainless steel reflector and moderator depends on the position in the core, 7 different radial reflector models were required.

For all fuel assemblies, the group constants are parametrized against the fuel temperature and the coolant density. Here are the values of these parameters:
- Coolant density: 0.8000 g/cm3, 0.90000 g/cm3, 0.92915 g/cm3, 0.996560 g/cm3;
- Fuel temperature: 525 K, 600 K, 700 K.
Radial reflectors are only generated with a coolant density of 0.92915 g/cm3.

KMACS automatically generates consistent inputs for SCALE-NEWT, steers the execution and stores the cross-sections in a database.

The tool PEMTY (Python External Meshing Tool with Yaml input) converts the group constants from the database into the NEMTAB-like format required by FENNECS.

9.6. FENNECS diffusion solution

The Finite ElemeNt NEutroniCS code FENNECS solves the steady state as well as the transient diffusion as well as the Simplified P3 (SP3) transport equations in the continuous Galerkin weighted residual finite element approach. Through its geometric flexibility, FENNECS can handle the more complex geometries of Small Modular Reactors (SMR). FENNECS has been coupled with the thermal-hydraulic system code ATHLET developed at GRS within the AC2 code package (Weyermann, Eschricht, & Wielenberg, 2023). PEMTY performs the meshing of the reactor.

FENNECS is still under development and has some limitations on which GRS is working on. Currently, it cannot perform pin power reconstruction. Pin-by-pin calculations are also under development.

Co-funded by the European Union
UK Research and Innovation
The Research Council of Norway
Project funded by

The model of the core in FENNECS consists of 25 axial meshes of around 5 cm each (3 meshes in the bottom reflector and 4 in the top reflector). Radially, each fuel assembly and reflector are modeled by a square divided into 16 triangles (see Figure 5) to obtain more accurate results.

The thermal hydraulic representation of the core in ATHLET is a parallel-channel open core model. Every fuel assembly is modeled as a parallel individual channel while all radial reflectors are modeled as a single channel. For coupled FENNECS/ATHLET simulations, a 1-by-1 mapping scheme between ATHLET and FENNECS is applied.

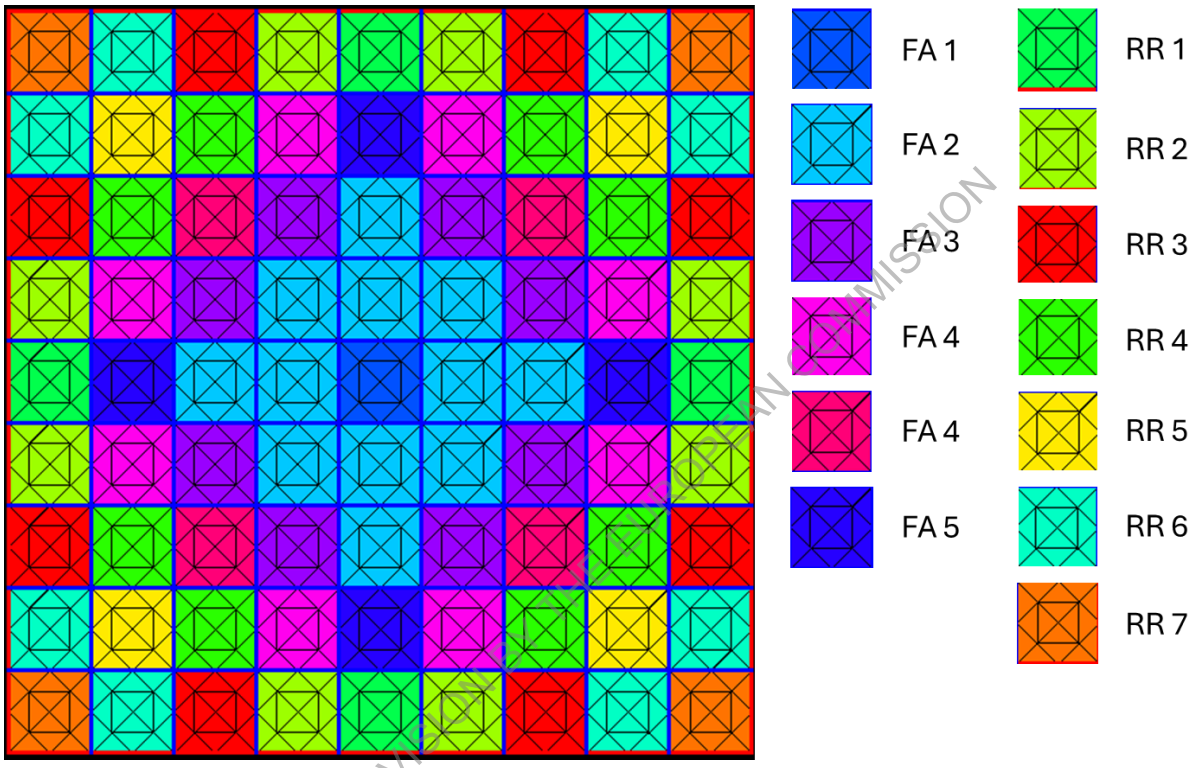

Figure 5. Radial core description in FENNECS. Picture created with PEMTY.

10. Results

10.1. ARO and critical states

Diffusion based results calculated with Ants, DYN3D and FENNECS for the ARO and critical states are compared against Serpent reference results in Table 8-Table 12 and Figure 6-Figure 10. Since fixed TH conditions were applied in these states, the use of neutronics-thermal hydraulics coupling was not required.

Co-funded by the European Union
UK Research and Innovation
The Research Council of Norway
Project funded by

Table 8. Effective multiplication factors estimated with Serpent in the ARO and critical states, and differences in reactivity between Ants/DYN3D/FENNECS and Serpent in pcm.

State	Serpent	Ants			DYN3D			FENNECS
		2g	4g	8g	2g	4g	8g	
ARO	1.07347	-195	-223	-194	-148	-262	-214	-770
Critical state	1.00275	-83	-162	-199	-8	-235	-220	-896

Table 9. Control rod group worths calculated with Serpent, and differences between Ants/DYN3D/FENNECS and Serpent in pcm.

Group	Serpent	Ants			DYN3D			FENNECS
		2g	4g	8g	2g	4g	8g	
All	20826	-114	66	184	-50	46	123	1083
S1	1020	1	3	10	-7	15	20	144
R2	2521	-24	-2	24	-42	25	41	159
R3	2354	-14	-6	8	-13	-1	10	149
S4	1390	33	17	16	48	4	7	175
R5	2760	-28	-8	17	-42	15	30	179
R6	3296	56	59	69	68	57	65	321
S7	1640	64	41	30	85	17	13	309
S8	1205	59	45	37	73	35	31	285

Table 10. Reactivity coefficients in the critical state.

Coefficient	Serpent	Ants			DYN3D			FENNECS
		2g	4g	8g	2g	4g	8g	
Fuel temperature (pcm/K)	-2.99	-2.90 (-3.1 %)	-2.92 (-2.2 %)	-2.95 (-1.4 %)	-2.93 (-1.8 %)	-2.94 (-1.7 %)	-2.99 (+0.0 %)	-2.45 (-17.9 %)
Coolant temperature (pcm/K)	-21.72	-21.31 (-1.9 %)	-21.56 (-0.7 %)	-21.66 (-0.3 %)	-21.33 (-1.8 %)	-21.53 (-0.8 %)	-21.68 (-0.2 %)	-23.04 (+6.1 %)

Deviation of the local normalized power from the reference shown in the following tables and figures is calculated as

(solver - reference) * 100

i.e. in per cent of the average assembly, pin or linear power. In the tables Root Mean Square (RMS) and Maximum (MAX) absolute differences are presented.

Table 11. Differences between relative axial, assembly and pin power distributions estimated with Ants/DYN3D/FENNECS and Serpent in the ARO state.

Distribution	Ants						DYN3D						FENNECS	
	2g		4g		8g		2g		4g		8g			
	RMS	MAX	RMS	MAX	RMS	MAX	RMS	MAX	RMS	MAX	RMS	MAX	RMS	MAX
Axial	0.7	1.7	1.0	2.1	1.1	2.1	0.7	1.8	1.0	2.1	0.8	1.7	0.8	1.7
Assembly	0.4	0.7	0.5	1.0	0.3	0.5	0.7	1.3	0.4	0.8	0.5	0.9	2.1	3.9
Pin	0.7	2.6	0.9	4.2	0.6	2.4	1.0	6.0	1.0	7.6	0.9	8.8	-	-

Table 12. Differences between relative axial, assembly and pin power distributions estimated with Ants/DYN3D/FENNECS and Serpent in the critical state.

Distribution	Ants						DYN3D						FENNECS	
	2g		4g		8g		2g		4g		8g			
	RMS	MAX	RMS	MAX	RMS	MAX	RMS	MAX	RMS	MAX	RMS	MAX	RMS	MAX
Axial	1.7	4.1	2.6	6.0	2.5	5.7	1.7	4.1	2.4	5.6	1.7	3.5	2.8	6.7
Assembly	0.8	1.6	0.9	2.1	0.7	1.5	1.1	1.9	0.8	1.8	0.9	2.0	2.4	5.9
Pin	1.2	3.9	1.5	5.9	1.1	3.8	1.5	6.6	1.4	8.0	1.2	8.2	-	-

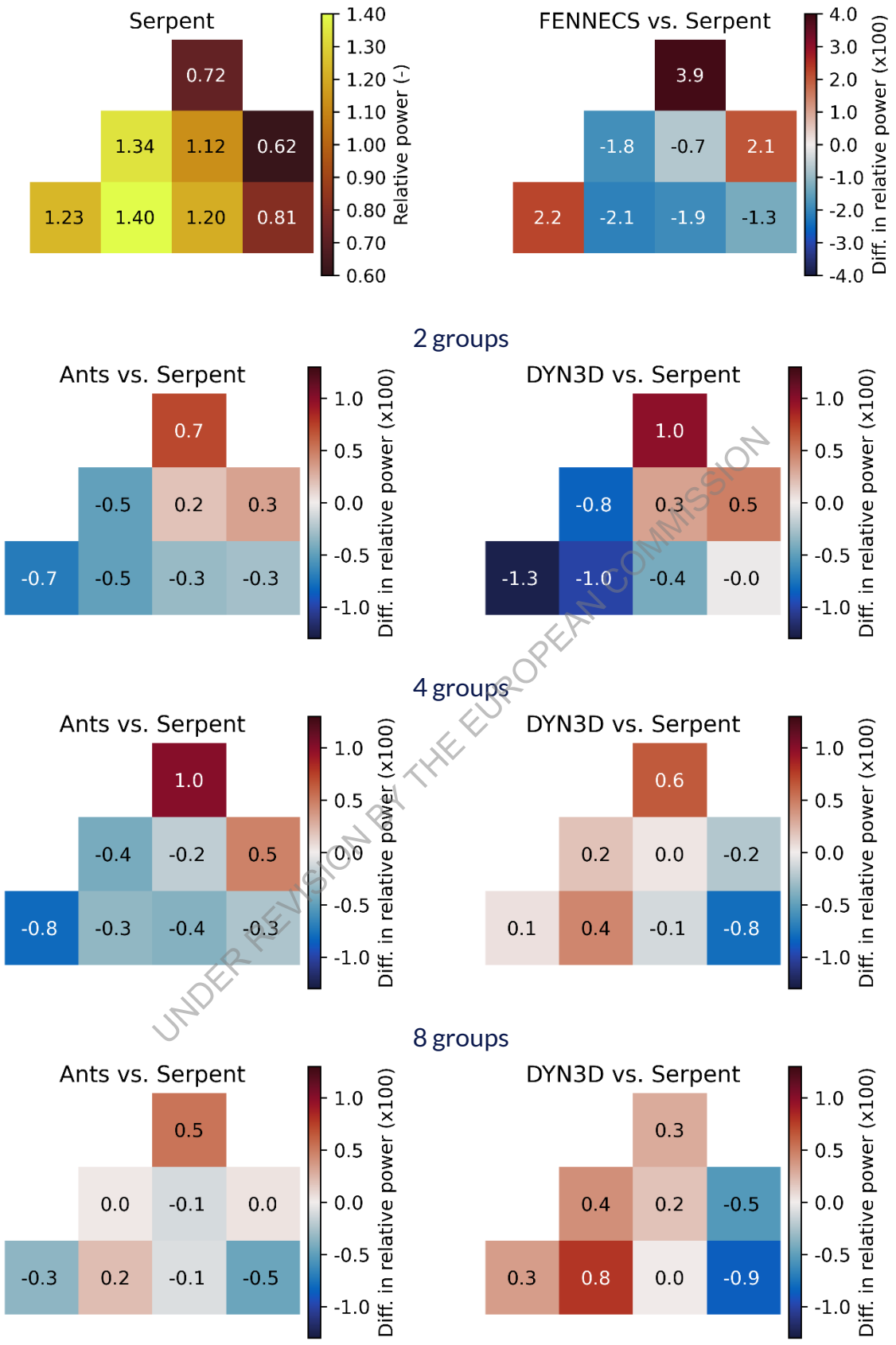

Figure 6. Comparison of assembly powers in the ARO state.

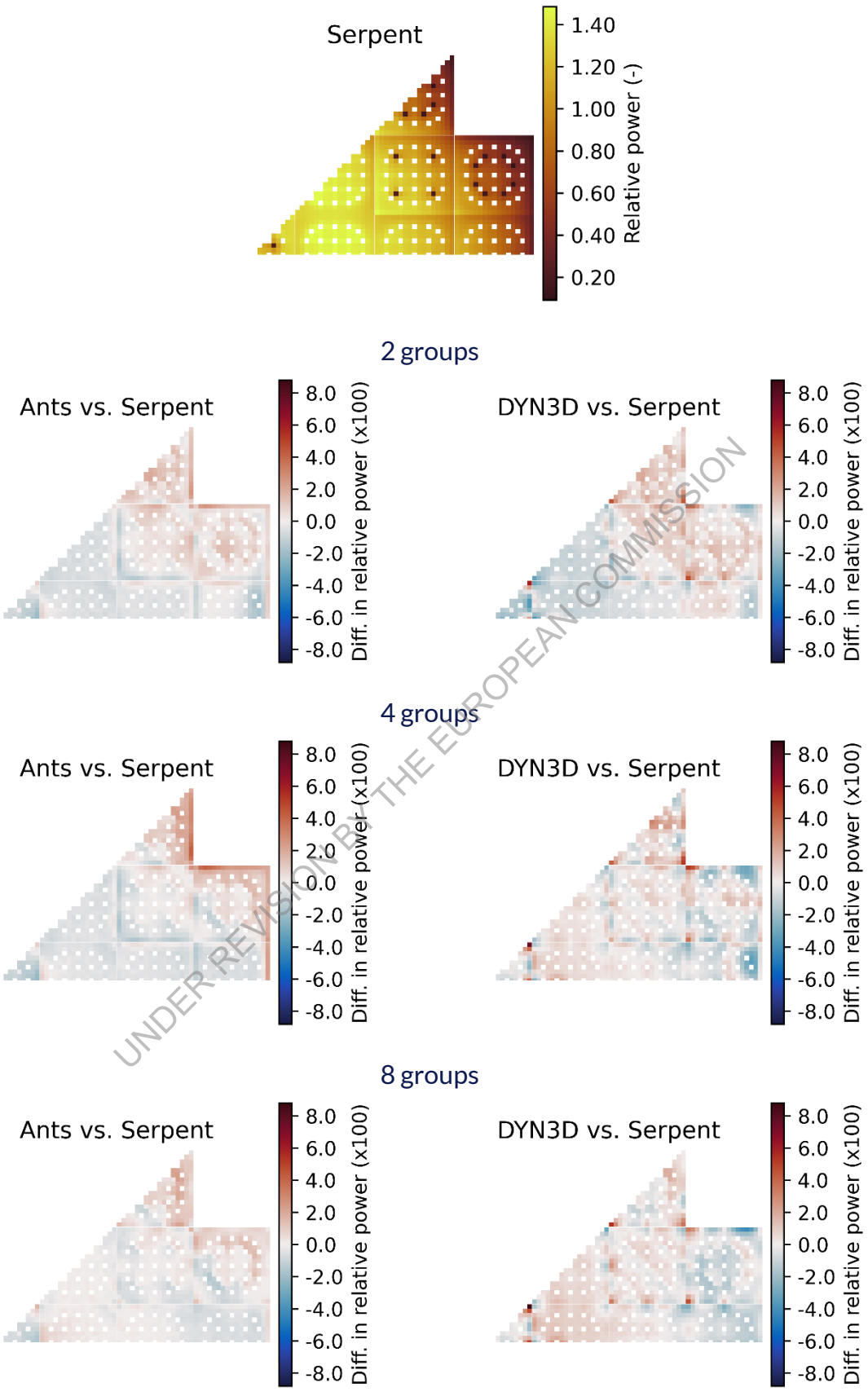

Figure 7. Comparison of pin powers in the ARO state.

Co-funded by the European Union
UK Research and Innovation
The Research Council of Norway
Project funded by

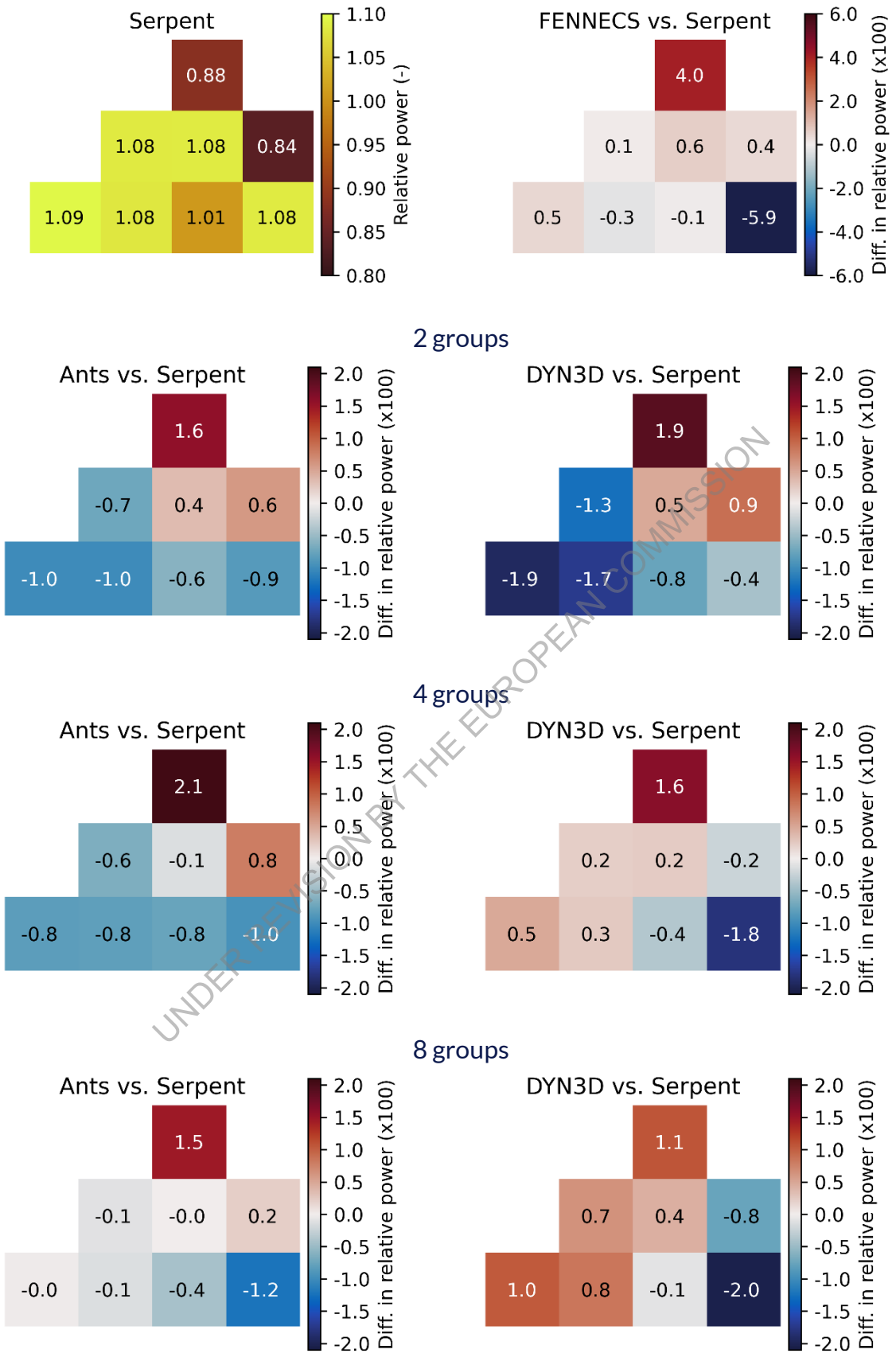

Figure 8. Comparison of assembly powers in the critical state.

Co-funded by the European Union
UK Research and Innovation
The Research Council of Norway
Project funded by

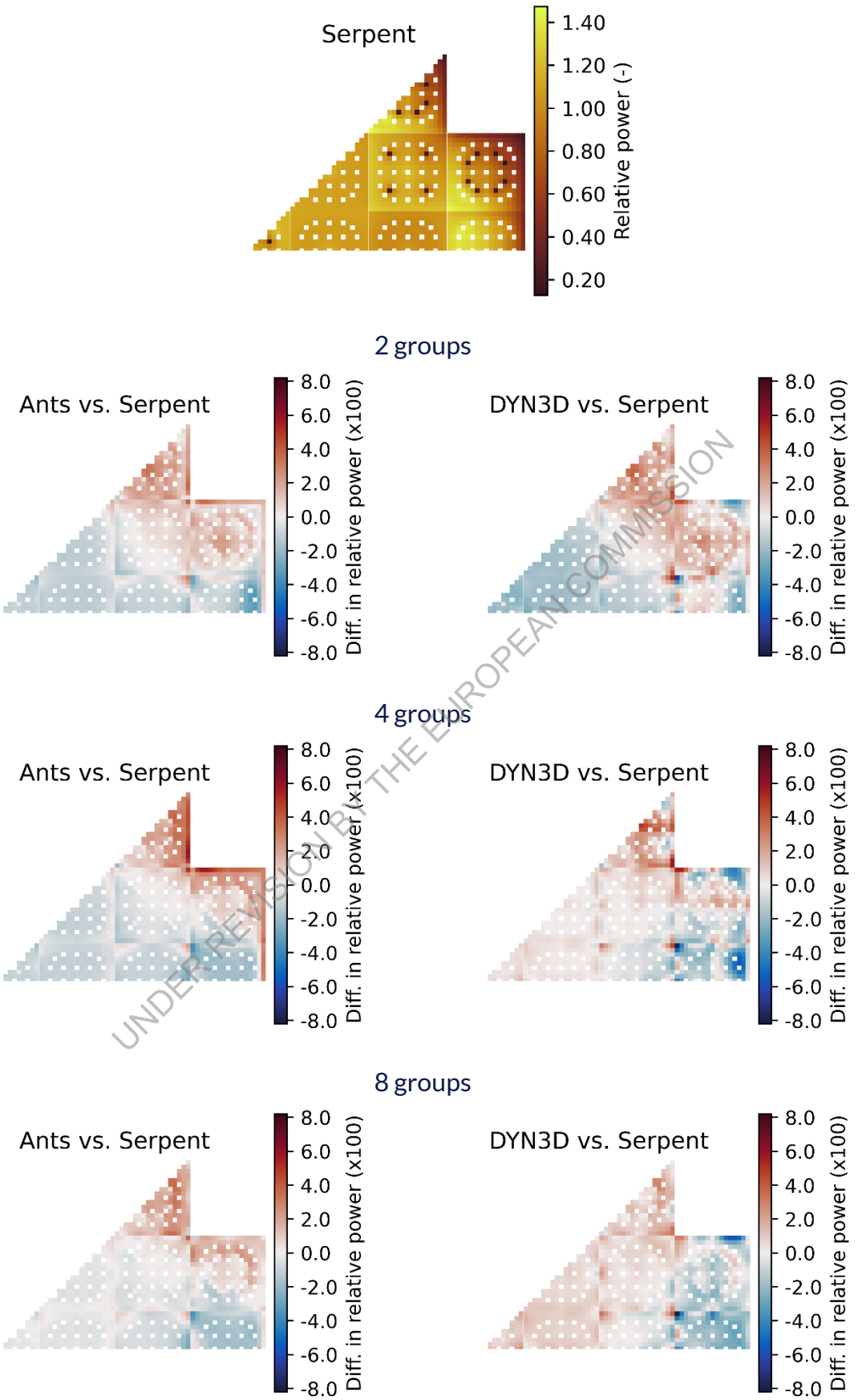

Figure 9. Comparison of pin powers in the critical state.

Co-funded by the European Union
UK Research and Innovation
The Research Council of Norway
Project funded by

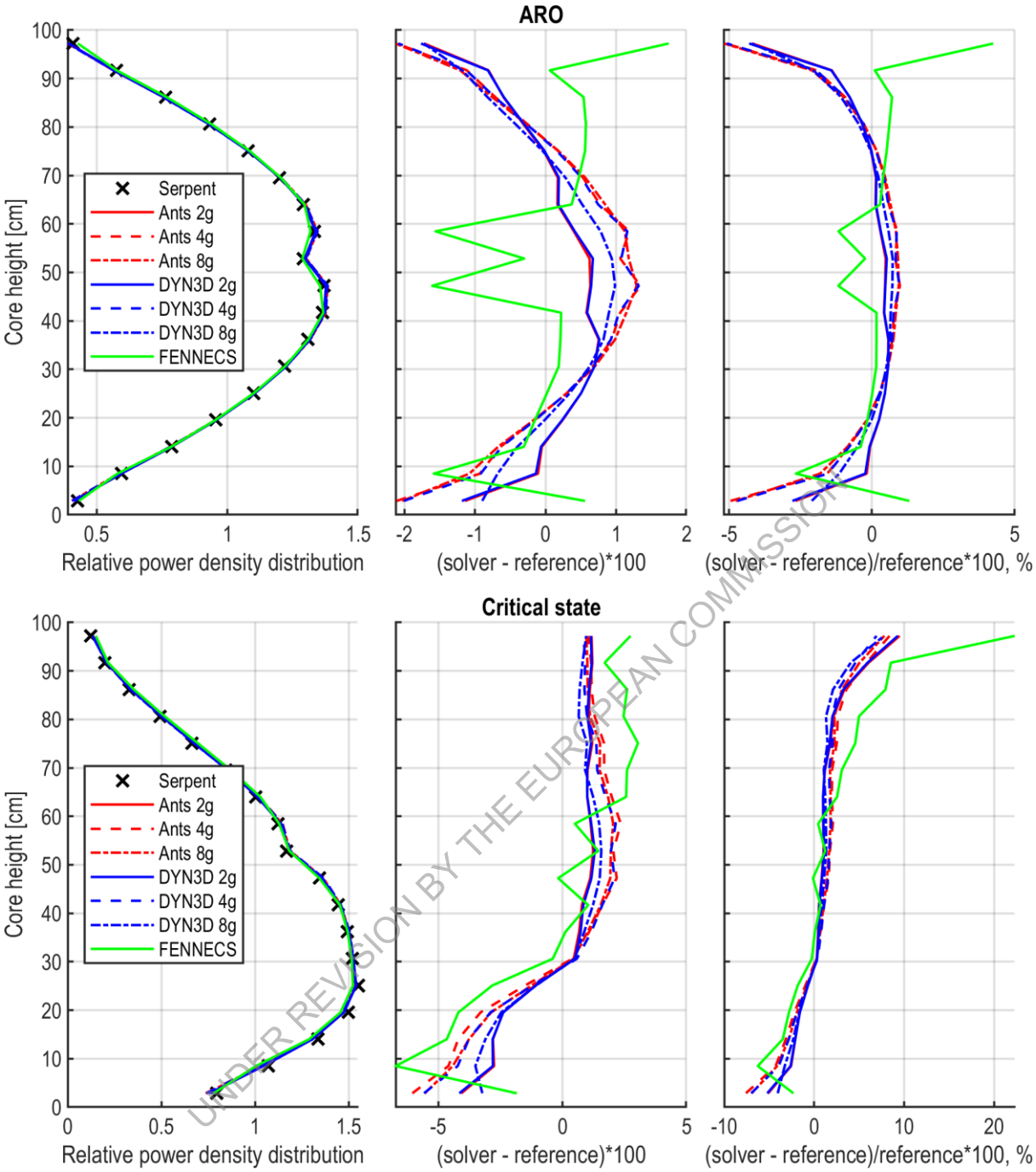

Figure 10. Comparison of axial power distributions in the ARO and critical states.

Co-funded by the European Union
UK Research and Innovation
The Research Council of Norway
Project funded by

10.2. HFP state

Diffusion based results calculated with Ants/SCF, DYN3D, and FENNECS/ATHLET for the HFP state are compared against Serpent/SCF reference results in Table 13-Table 14 and Figure 11-Figure 13.

Table 13. Effective multiplication factor estimated with Serpent in the HFP state, and differences in reactivity between Ants/DYN3D/FENNECS and Serpent in pcm.

Serpent	Ants			DYN3D			FENNECS
	2g	4g	8g	2g	4g	8g	
1.00154	2	-67	-107	-206	-412	-412	-875

Table 14. Differences between relative axial, assembly and pin power distributions estimated with Ants/DYN3D/FENNECS and Serpent in the HFP state.

Distribution	Ants						DYN3D						FENNECS	
	2g		4g		8g		2g		4g		8g			
	RMS	MAX	RMS	MAX	RMS	MAX	RMS	MAX	RMS	MAX	RMS	MAX	RMS	MAX
Axial	1.8	3.7	2.5	5.4	2.4	5.1	0.6	1.7	0.9	3.0	0.5	1.1	4.5	9.0
Assembly	0.7	1.1	0.7	1.5	0.4	1.0	1.2	2.0	0.8	1.7	0.8	1.7	1.9	4.4
Pin	1.0	3.5	1.2	5.1	0.8	3.4	1.6	6.0	1.5	6.8	1.3	6.5	-	-

Co-funded by the European Union
UK Research and Innovation
The Research Council of Norway
Project funded by

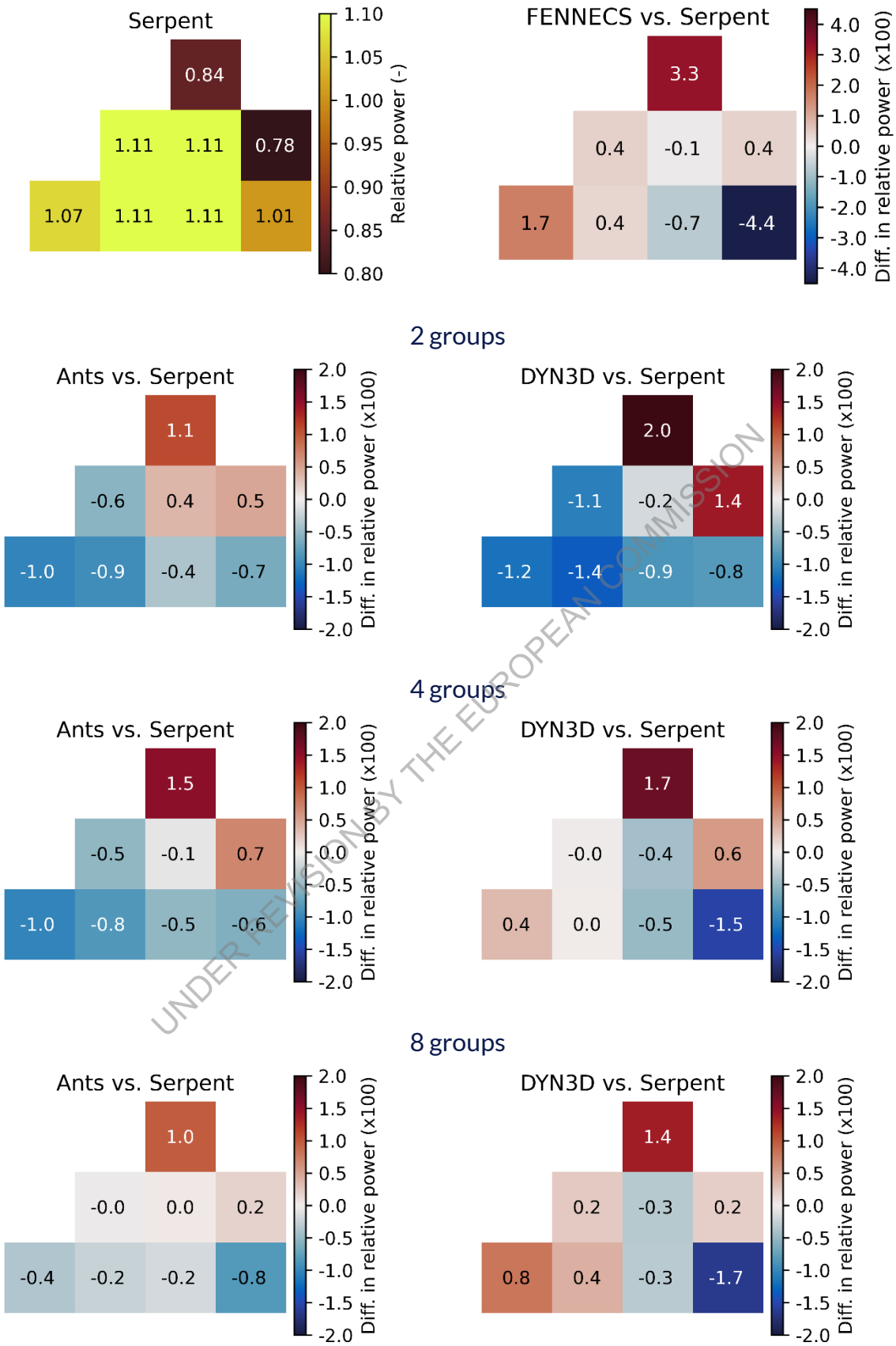

Figure 11. Comparison of assembly powers in the HFP state.

Co-funded by the European Union
UK Research and Innovation
The Research Council of Norway
Project funded by

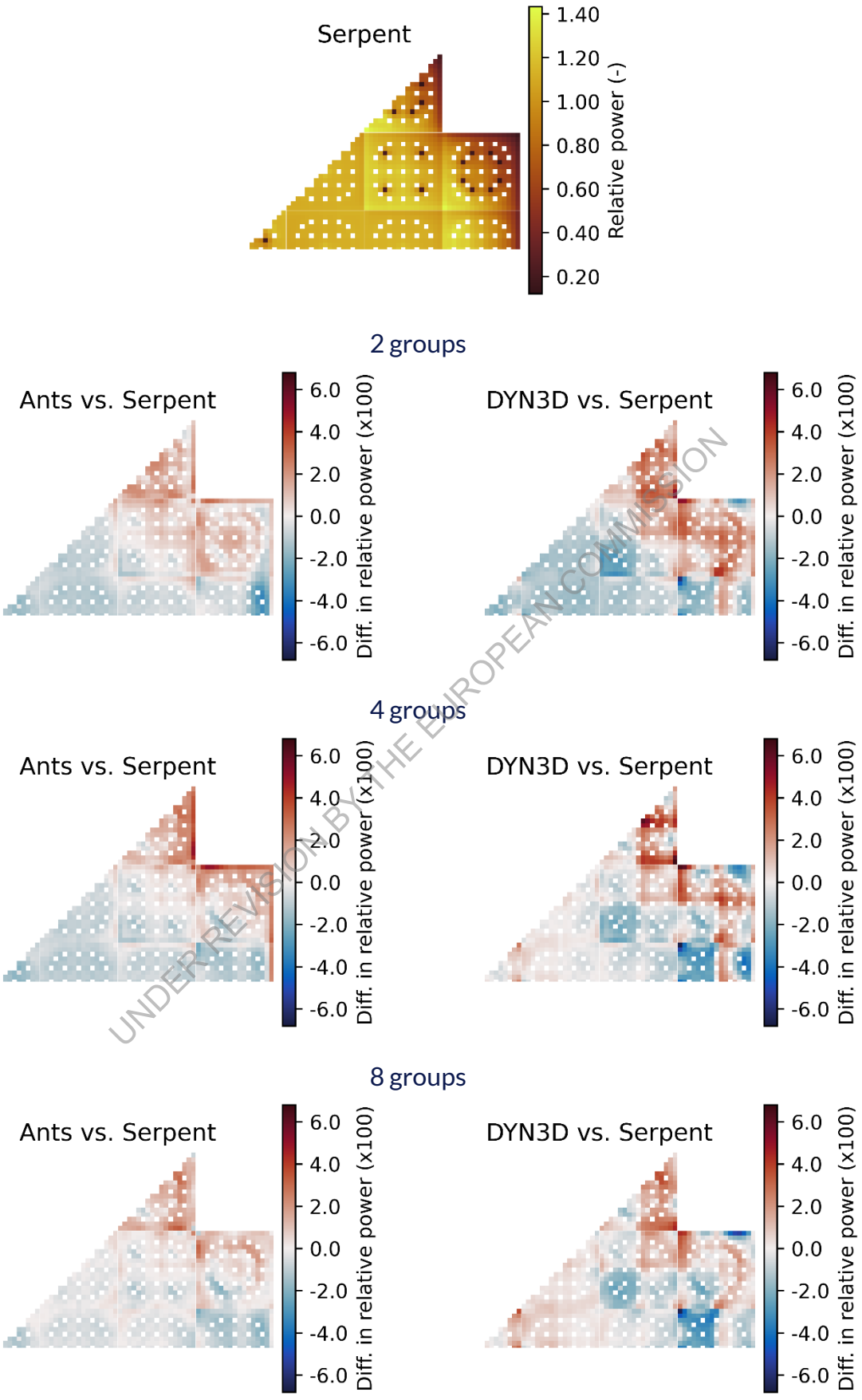

Figure 12. Comparison of pin powers in the HFP state.

Co-funded by the European Union
UK Research and Innovation
The Research Council of Norway
Project funded by

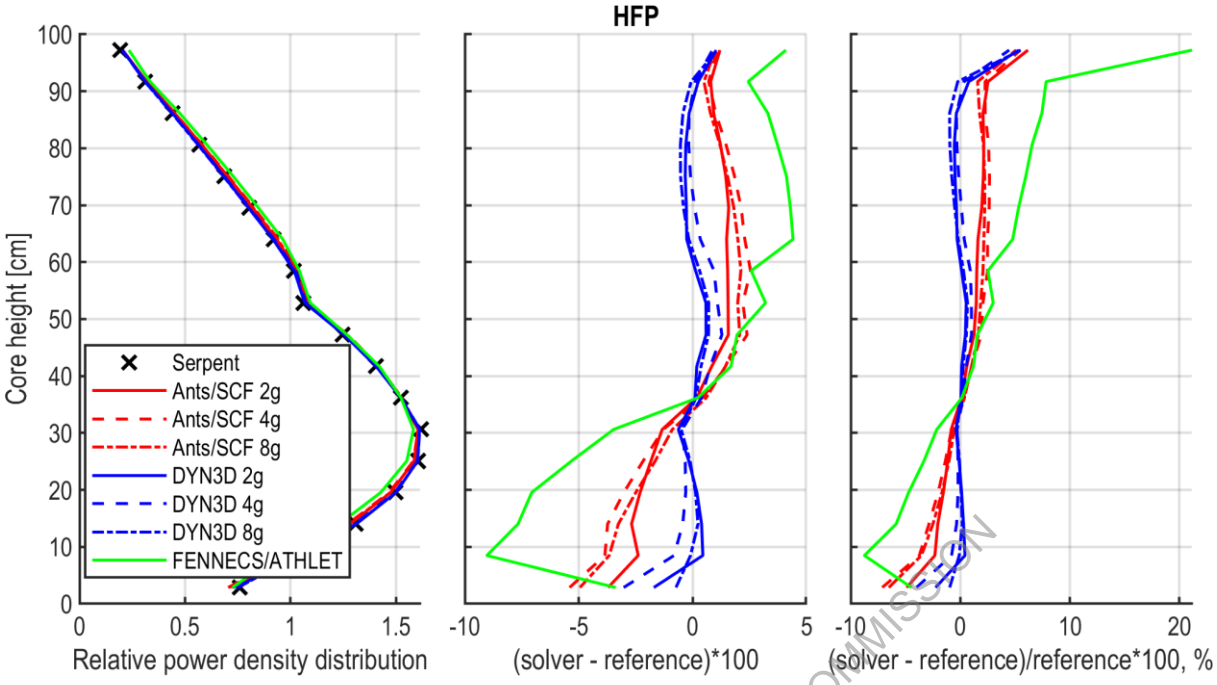

Figure 13. Comparison of axial power distributions in the HFP state.

10.3. Discussion

Here, the results obtained with Ants and DYN3D are analysed separately from the ones of FENNECS because the discrepancies between FENNECS and Serpent were significantly larger than those between Ants, DYN3D and Serpent. Observations from the results shown in Table 8-Table 10: Core reactivity is best predicted by the two nodal codes (DYN3D and Ants) using 2-group energy structure, with the maximum error below 200 pcm, and the worst result is obtained with 4 groups, with maximum error of approximately 260 pcm. The reactivity coefficients and control rod group worths obtained by the nodal codes are in good agreement with the Serpent reference, with 4- and 8-group results slightly better than 2-group results.

The agreement of nodal codes with the reference ARO and critical state solutions (see Table 11-Table 12 and Figure 6-Figure 9) in assembly power distribution is within 2 % with maximum RMS difference of approximately 1 %. For pin powers, Ants differences are within 6 % with RMS differences of less than 1.5 %, while DYN3D differences are within 9 % with RMS differences of less than 1.5 %. No clear conclusion can be derived about the influence of the energy groups number: for Ants, the worst results are obtained with 4-group library, and 2- and 8-group results are similar to each other, while for DYN3D the best results in pin powers are obtained with the 2-group library.

Axial power distributions in the ARO and critical states (see Figure 10) obtained with DYN3D and Ants reproduce the Serpent reference closely, with minimal difference between two nodal codes. The highest errors are located at the core periphery near the axial reflectors, up to 2 % in ARO case and up to 5 % in the critical case.

The HFP results are influenced by the differences in TH solvers and TH model radial discretisation: Serpent/SCF is pin-resolved, while Ants/SCF and DYN3D models are quarter-assembly resolved. Another important difference is the fact that DYN3D TH solver considers each channel as isolated, while SCF allows for mass and energy exchange between channels. Core reactivity (Table 13) is predicted best by Ants/SCF, with an error of 2 pcm using 2-group library and up to 100 pcm with more groups. DYN3D produced 200 pcm error with 2-group library and more than 400 pcm with 4 and 8 groups. Differences in the radial power distribution (see Table 14 and Figure 11-Figure 12) for Ants/SCF are up to 1.1 % in assembly power and up to 3.5 % in pin power for 2 groups, and 4-group maximum errors are 1.5 % and 5.1 %, respectively. For DYN3D the differences for 2 groups are within 2 % for assembly power and within 6 % for pin power, with more groups producing slightly better agreement in assembly powers and slightly worse in pin powers. In the axial power distribution (Figure 13) the difference between Ants/SCF and DYN3D is more pronounced than in the neutronics only states, probably due to the influence of different TH solutions.

Concerning FENNECS results, it is observed that overall FENNECS calculations are showing larger discrepancies than DYN3D and Ants calculations. In the ARO configuration, FENNECS underestimates the core reactivity by approximately 800 pcm, which is a relatively large discrepancy. A plausible explanation for this deviation lies in the current modelling of the radial reflector, which is likely insufficiently accurate. This interpretation is further supported by the radial power distribution obtained for the ARO case: FENNECS overestimates the power in the fuel assemblies located at the edge of the core (up to 3.9 %), highlighting deficiencies in the treatment of neutron reflection at the core boundary. No specific treatment or correction of the group constants are applied for this region. Improving radial reflector modelling and investing a proper treatment is therefore identified as a priority for future developments.

More generally, FENNECS underestimates the multiplication factor in all analysed cases. However, the control rod worths are only moderately overestimated, by about 150 pcm for the inner control rods and approximately 300 pcm for the outer control rods. These results suggest that the main source of the bias is not related to the control rod modelling. Consequently, it can be expected that a more accurate representation of the radial reflectors would significantly reduce the discrepancy in the multiplication factor.

Concerning the critical state and the HFP state, in a similar way, FENNECS underestimates the core reactivity by 900 pcm and 880 pcm, respectively, which is in the same order of magnitude as in the ARO state. In both states, FENNECS shows similar discrepancy in the shape of the radial power distribution: while FENNECS can predict well the power in the middle of the core (less than 0.5 % and 1.7 % discrepancy in the critical state and in the HFP state, respectively), the assembly powers at the edge of the core are either underestimated by 5.9 % and 4.4 %, or overestimated by 4.0 % and 3.3 % in the critical state and in the HFP state, respectively. It is expected that by improving the radial reflector modelling, FENNECS can predict the multiplication factor and radial power distribution better.

An evaluation of the calculated reactivity coefficients reveals noticeable discrepancies between the reference data and the results obtained with FENNECS. The fuel temperature reactivity coefficient shows a discrepancy of 17.9 %. This deviation is

significant and suggests a strong sensitivity of the results to the modelling assumptions, nuclear data, or numerical methods used in the calculation. The moderator density reactivity coefficient exhibits a smaller discrepancy of 6.1 %. While this difference is less pronounced than the one observed for the fuel temperature coefficient, it remains non-negligible. This shows the need for a more appropriate calculation scheme for group constants generation.

11. Conclusions

The beginning of initial cycle core of LDR lite was modelled by VTT, HZDR and GRS using nodal diffusion codes Ants and DYN3D and a new finite element neutronics code FENNECS. Results are compared with the Serpent Monte Carlo reference solution. For the hot full power state, the thermal feedback was taken into account by coupled solutions using Ants/SCF, DYN3D, FENNECS/ATHLET and Serpent/SCF.

Nodal codes have shown close agreement with the reference: with 2-group libraries the deviations in reactivity are limited to 200 pcm, in assembly powers to 2 % and in pin powers to 7 %.

The influence of the number of energy groups in the few-group library of nodal codes was also investigated. Overall, the best agreement with the reference was achieved using 2-group libraries, with 4- and 8-group libraries showing no notable improvement and, in some cases, even produced less accurate results.

FENNECS is currently under development and is not yet able to solve all benchmark tasks. In particular, pin power reconstruction is not yet implemented but it is foreseen for the next development phase of the FENNECS code. In the short term, direct pin-by-pin simulations for a small part of the core (quarter symmetry) can be performed but group constants must be generated consequently. It has been also seen that the use of simplified reflector modelling for group constant generation leads to noticeable deviations from reference solutions. Ongoing developments, including improvements in modelling fidelity and cross-section methodologies, are expected to enhance the predictive accuracy of the code. The benchmark results therefore highlight the current limitations of FENNECS.

Co-funded by the European Union
UK Research and Innovation
The Research Council of Norway
Project funded by

12. Bibliography

Bousquet, J., Seubert, A., & Henry, R. (2020). New finite element neutron kinetics coupled code system code system FENNECS/ATHLET for safety assessment of (very) smal and Micro Reactors. *Journal of Physics: Conference Series*, 1689.

Henry, R., Bousquet, J., & Seubert, A. (2024). Implementation of the discontinuous Galerkin method inte FENNECS and other new improvements for LWR analysis. *PHYSOR 2024: International Conference on Physics of Reactors.* San Francisco, CA, USA: American Nuclear Society.

Imke, U. (2019). User manual for SUBCHANFLOW 3.6.1.

Imke, U., & Sanchez, V. H. (2012). Validation of the subchannel code SUBCHANFLOW using the NUPEC PWR tests (PSBT). *Science and Technology of Nuclear Installations*(2012).

Leppänen, J., Valtavirta, V., Rintala, A., & Tuominen, R. (2025). Status of Serpent Monte Carlo code in 2024. *EPJ Nuclear Sci. Technol.*(11), 3.

Liu, Z., Smith, K., & Forget, B. (2018). Group-wise tally scheme of incremental migration area for cumulative migration method. *Proceedings of the PHYSOR 2018*, (pp. 2512-2523).

Rohde, U. e. (2016). The reactor dynamics code DYN3D – models, validation and applications. *Progress in Nuclear Energy*, 170-190.

Sahlberg, V., & Rintala, A. (2018). Development and first results of a new rectangular nodal diffusion solver of Ants. *Proceedings of the PHYSOR 2018*, (pp. 3861-3871).

Seubert, A., lo Muzio, S., Elts, E., & Bousquet, J. (2026). The Neutron Kinetics Code FENNECS for the Safety Assessment of MMRs, SMRs and Innovative Reactor Concepts. *PHYSOR 2026 - The International Conference on Physics of Reactors.* Turin, Italy.

Smith, K. (2017). Nodal diffusion methods and lattice physics data in LWR analyses: Understanding numerous subtle details. *Progress in Nuclear Energy*(101), 360-369.

Tuominen, R., & Bilodid, Y. (2026). Modelling of the Initial Core of the LDR Lite Benchmark within the EU-funded EASI-SMR Project. *PHYSOR 2026 - The International Conference on Physics of Reactors.* Turin, Italy.

Valtavirta, V., & Tuominen, R. (2025). *D7.2 Specifications of the LDR lite core at BOC fresh conditions.* EASI-SMR project.

Weyermann, F. C., Eschricht, D., & Wielenberg, A. (2023). *AC2-2023 User Manual, GRS- P-15/Vol. 0.* Gesellschaft für Anlagen- und Reaktorsicherheit (GRS).

Wieselquist, W. A., & Lefebvre, R. A. (2024). *SCALE 6.3.2 User Manual.* UT-Battelle, Oak Ridge National Laboratory.

Zilly, M., & Périn, Y. (2018). *KMACS Validation Report, Technical Report GRS-P-8/Vol. 2, Rev.* GRS gGmbH.

Co-funded by the European Union
UK Research and Innovation
The Research Council of Norway
Project funded by